Journal of Engineering Sciences

Vol 11, Issue 2, FEB/2020
ISSN NO:0377-9254

Energy Harvester from MEMS based Piezoelectric

M. Sreenivasulu[1]

[1]Research Scholar, ECE Dept

JNTUH, Hyderabad

Assoc. Professor, Samskruti College of Engg & Tech,Hyderabad
srinuvas42@gmail.com

B.Sowbhagya[2]

Assistant Professor,

Ballari Institute Of Technology And Management,

Ballari, Karnataka,India

Abstract— **Abstract:** Piezoelectric energy harvester (PEH) is emerging as a novel device which can convert mechanical energy into electrical energy. It is mainly used to collect ambient vibration energy to power sensors, chips and some other small applications. This paper first introduces the working principle of PEH. Then, the paper elaborates the research progress of PEH from three aspects: piezoelectric materials, piezoelectric modes and energy harvester structures. Piezoelectric material is the core of the PEH. The piezoelectric and mechanical properties of piezoelectric material determine its application in energy harvesting. There are three piezoelectric modes, d_{31}, d_{33} and d_{15}, the choice of which influences the maximum output voltage and power. Matching the external excitation frequency maximizes the conversion efficiency of the energy harvester. There are three approaches proposed in this paper to optimize the PEH's structure and match the external excitation frequency, i.e., adjusting the resonant frequency, frequency up-converting and broadening the frequency bandwidth. In addition, harvesting maximum output power from the PEH requires impedance matching. Finally, this paper analyzes the above content and predicts PEH's future development direction.

Keywords— energy harvesting; piezoelectric material; piezoelectric modes; resonant frequency

I. INTRODUCTION

In recent years, wireless sensor network technology has been widely used in environmental monitoring, health care, urban temperature detection, agricultural production and other fields [1–6]. The main power supply for sensor nodes still relies on chemical battery, which offers limited energy storage. Further, as the sensor nodes are widely distributed, it would be difficult to replace and maintain the battery.

Specifically, energy harvesting technology converts other forms of energy into electrical energy, which is then collected to power the circuit or device [7]. Several forms of energy exist in the environment, such as mechanical energy, thermal energy, nuclear energy, solar energy, chemical energy, etc. [8]. Among them, mechanical energy is the most widely distributed.

According to the different principles, mechanical energy harvester can be divided into three categories, i.e., electromagnetic energy harvester, electrostatic energy harvester and piezoelectric energy harvester (PEH) [9–13]. Comparing electromagnetic and electrostatic ones, PEH has a higher energy density and is suitable to harvest vibration energy [14].

Generally, PEH can be classified into three groups: (1) macroscale; (2) MEMS scale; and (3) nanoscale. The size of a PEH affects a variety of parameters such as its weight, fabrication method, achievable power output level, and potential application areas. For example, nanoscale PEH can be motivated by rubbing, pressing or pulling [15–17]. It is suitable to harvest energy from human motion. As to larger scale PEHs, they are mainly motivated by ambient vibration, especially vibration with fixed frequency. At present, there are still problems that limit the application of PEH: (1) the power loss in rectification circuit caused by the low output voltage [18]; (2) the narrow working frequency bandwidth of the energy harvester [9,19,20]; and (3) the mismatch of the frequency between the PEH and the environment [21,22].

This article mainly discusses the MEMS scale PEH. The following section introduces a general model of energy harvester and describes the research progress of PEHs from three aspects: piezoelectric materials, piezoelectric modes and energy harvesters' structure. These contents are analyzed in Section 3. Section 4 predicts the future development of PEHs.

II. RESEARCH PROGRESS OF PEH

In 2004, Sodano et al. [23] first developed the model of the PEH, which consists of cantilever beam, piezoelectric material and electrodes. The piezoelectric material is interfaced to the cantilever beam near the fixed end, and the electrode is connected to the piezoelectric material to derive the current. When the external excitation load is applied to the base of the energy harvester, the cantilever beam moves with it. Thus, the piezoelectric material is subjected to compression deformation and a voltage difference occurs on the surface of the piezoelectric material. By designing appropriate rectifier circuit to be connected to the electrodes, the current generated from the PEH is finally exported and stored.

2.1. General Model of Energy Harvester

In 1995, Williams and Yates [24] proposed a model which was based on linear system theory to simulate the energy harvester. The model consists of a seismic mass, m, a spring, k, and damping, d. The model can accurately simulate the electromagnetic energy harvester mentioned in their article, but it is only feasible when the damping and stiffness are linear. For PEHs, the model needs to be changed because the impact of the electrical system on the mechanical system is not linear. Even so, important conclusions of the model can be promoted on PEHs. Based on this, Roundy [25] further decomposed the damping into electrically induced damping and mechanical damping in 2002. The improved mass–spring–damping system is shown in Figure 1. The system consists of a mass m, a spring with a stiffness k as well as the electrically induced damping b_e and the mechanical damping b_m. While applying an external sinusoidal displacement load $y(t) = Y_0 \cos(wt)$ with the amplitude Y_0 on the model, the relative motion of the mass with respect to the housing would be z(t).

The differential equation of the model can be expressed by Equation (1):

$$m\ddot{z} + (b_e + b_m)\dot{z} + kz = m\ddot{y} \quad (1)$$

$$P = kz\dot{y} + z$$

Combining Equations (1) and (2), the power converted can be expressed as:

$$P_C = \frac{m\zeta_e w_n w^2 \left(\frac{w}{w_n}\right)^3 Y_0^2}{\left(1 - \left(\frac{w}{w_n}\right)^2\right)^2 + \left(2\zeta_T \frac{w}{w_n}\right)^2}$$

where z_e represents electrical damping ratio; z_T indicates the combined damping ratio ($z_T = z_e + z_m$); w is the input frequency; and w_n suggests the natural frequency (or resonant frequency) of the model.

When the model's resonant frequency matches the input frequency, the energy harvester can obtain the maximum conversion energy, as shown in Equation (4). Furthermore, the equation also shows that as the input frequency increases, the power converted P_C rises.

When the model's resonant frequency matches the input frequency, the energy harvester can obtain the maximum conversion energy, as shown in Equation. Furthermore, the equation also shows that as the input frequency increases, the power converted P_C rises

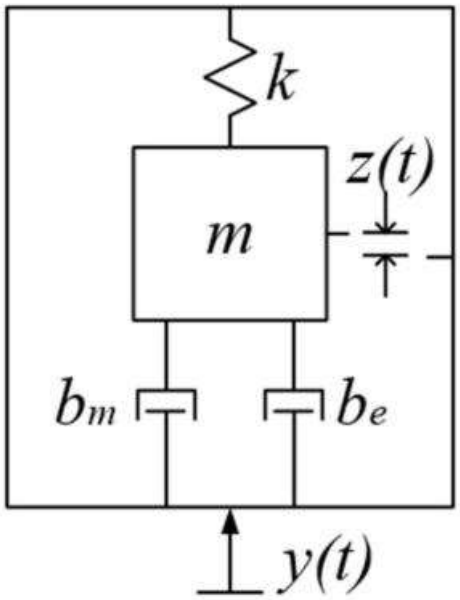

Figure 1. Schematic of spring–mass–damping system.

Research Progress of Piezoelectric Materials

Piezoelectric material is a class of solid materials that can accumulate electric charge in response to applied mechanical stress. In 1880, Pierre and Jacques Curie [26] discovered the piezoelectric effect of quartz crystals. Since then, more piezoelectric materials have been found. These crystals have the characteristic of low crystal symmetry. The crystal is also prone to polarization.

Usually at elevated temperatures, polycrystalline ferroelectric materials may be brought into a polar state by applying a strong electric field [27], as shown in Figure 2. For a single crystal, it does not contain domains and is said to be in a single-domain or monodomain state.

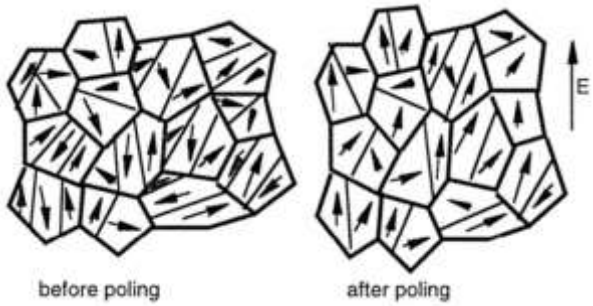

Figure 2. A polycrystalline ferroelectric is before and after poling. Reprinted by permission from Damjanovic.

The constitutive equations for piezoelectric material, which describe the direct piezoelectric effect, are shown in Equations (5) and (6):

$$d = s/Y + dE \quad (5)$$

$$D = \#E + ds \quad (6)$$

where *d* represents the mechanical strain, *s* the mechanical stress, Y the Young's modulus, D the charge density, E the electric field, # the dielectric constant, and d the piezoelectric constant.

Equations (5) and (6) are coupled together via the piezoelectric coupling term d. They provide the mechanism for power generation from vibrations. The voltage generated by the piezoelectric material is proportional to the distance between electrodes L, voltage constant g_{ij} and stress s_{xx} as shown in Equation (7) [28]. The voltage constant g_{ij} can be derived from Equation (8), where d_{ij} is the piezoelectric constant, $\#_r$ is the relative dielectric constant and $\#_0$ is the permittivity of vacuum [29]

$$V_{oc} = s_{xx} g_{ij} L \quad (7)$$

$$g_{ij} = \frac{d_{ij}}{\#_r \#_0} \quad (8)$$

From Equations (7) and (8), output power is affected by piezoelectric material parameters, the voltage constant g_{ij} and the piezoelectric constant d_{ij}. Therefore, the d-g product is an important characteristic of piezoelectric materials.

Piezoelectric materials are roughly divided into inorganic and organic matters. At present, the common inorganic piezoelectric materials are piezoelectric single crystals and piezoelectric ceramics (polycrystalline). Organic piezoelectric materials generally refer to piezoelectric polymers such as polyvinylidene fluoride (PVDF) [30]. In recent years, some organic nanostructures through special processing, such as nanotubes [15], nanowires [16], and nanoparticles [17], are also found to have piezoelectric activity.

Among these materials, nanostructures with high effective piezoelectric constant are used for energy harvesting in nanoscale PEHs. Recent reports have shown high conversion efficiency in nanoscale PEHs. Besides, nanostructures are lead-free and environment friendly. For larger scale PEHs, piezoelectric ceramics is the largest material group for piezoelectric devices, while piezoelectric polymer demonstrates fastest growth due to its light weight and small size. In addition, the piezoelectricity and dielectric constant of the piezoelectric single crystal are lower than that of piezoelectric ceramics. By contrast, although the piezoelectric polymer has low density, low impedance, the strain constant and the piezoelectric constant is relatively low. At present, some people are trying to apply piezoelectric polymer to nanoscale PEHs [31,32]. Comparing the above two materials, piezoelectric ceramics have some advantages: (1) the piezoelectric constant and dielectric constant are higher; (2) higher plasticity of the shape; and (3) material composition is easy to be controlled, thereby improving its prospects. However, it should be noted that the stability and energy consumption of the piezoelectric materials still need to be further studied. Overall, the piezoelectric material has great potential for development and application.

To protect the environment, piezoelectric ceramics are now developing towards lead-free direction such as $NaNbO_3$ and $K_{0.5}Na_{0.5}TiO_3$ [33]. The sintering of these kinds of material is a challenge. In 2005, Guo et al. [34] prepared $(Na_{0.5}K_{0.5})NbO_3$-$LiTaO_3$ using conventional mixed oxide route and found it was a good lead-free piezoelectric ceramic. Its piezoelectric constant d_{33} was up to 200 pC/N, and the plane electromechanical coefficient K_p reached 36%. The doping amount of $LiTaO_3$ affected the phase of the material. In 2006, Li et al. [35] studied $(Na_{0.5}K_{0.5})NbO_3$ by using the spark plasma sintering (SPS) method with advantage of low-temperature sintering. The Curie temperature was 395 C and the highest dielectric constant $\#_r$ was 606, but the piezoelectric constant (148 pC/N) was lower than that in the report of Guo et al. In the same year, Lin et al. [36] studied the $[Bi_{0.5}(Na_{1-x-y}K_xLi_y)_{0.5}]TiO_3$. They found that the piezoelectric constant (231 pC/N) and the maximum dielectric constant (1190) reached the peak when x/y = 0.2/0.1. It should be noted that doping could increase the Curie temperature or the quality of grain growth, but d_{33} and K_p would decrease slightly [37,38]. In 2016, Shi et al. [39] studied the effect of Fe on the piezoelectric properties and fatigue behavior of $(Bi_{0.5+x/2}Na_{0.5-x/2})_{0.94}$-$Ba_{0.06}Ti_{1-x}Fe_xO_3$ (BNBT-xFe). They found that the induction of Fe in the electric field resulted in the decrease in the ferroelectric-relaxor transition temperature, but the strain would increase. In addition to doping, optimizing the preparation of materials could also improve the performance of piezoelectric materials [40].

Table 1 lists some parameters of the piezoelectric materials. From the table, traditional piezoelectric ceramics, lead zirconate titanate (PZT), mostly have high piezoelectric constants. The piezoelectric properties of lead-free piezoelectric materials can be enhanced by doping. There are many reports on doping showing the importance of doping for piezoelectric materials. The max piezoelectric constant d_{33} stood at 295 pC/N. The commonly used preparation method is the solid-state liquid-phase sintering technique. In addition, the planar K_p and thickness K_t electromechanical coupling coefficients were between 30% and 50%. However, the maximum dielectric permittivity differed significantly. The reason for this might because of the difference properties of the piezoelectric ceramic or ratio.

Table 1. Comparison of some parameters of piezoelectric material.

Materials	d_{31}	d_{33} (pC/N)	K_p (%)	# r	T_{Curie} (C)	Reference
PZT-2	60.2	152	47	-	370	
PZT-4	123	289	58	-	328	
PZT-5A	171	374	60	-	365	
PZT-5H	274	593	65	-	193	
PZT-8	37	225	51	-	300	
$(Na_{0.5}K_{0.5})NbO_3$-$LiTaO_3$	-	200	36	570	-	[34]
$(Na_{0.5}K_{0.5})NbO_3$	-	148	38.9	606	395	[35]
$[Bi_{0.5}(Na_{1-x-y}K_xLi_y)_{0.5}]TiO_3$	-	231	41.0	1190	-	[36]
0.69BiFeO–0.04Bi(ZnTi)O–0.27BaTiO (MoOdoped)	-	145	41.0	-	510	[37]
$Li_{0.058}(K_{0.480}Na_{0.535})_{0.966}(Nb_{0.9}Ta_{0.1})O_3$ (ZnO doped)	-	272	44	5081	395	[38]
$Bi_{0.5}(Na_{0.68}K_{0.22}Li_{0.1})_{0.5}TiO_3$	-	295	-	2720	-	[42]
((Ba0.90Ca0.10)(Ti0.85Zr0.15)O3 doped)						
(Bi0.5Na0.5)TiO3(BaTiO3doped)	37	180	-	1557	-	[43]
((Na0.535K0.48)NbO3(LiNbO3 doped)		150	50	5500	470	[44]
0.995(K0.5Na0.5)1 xLixNbO3–0.005BiAlO3		182	37.5	5000	450	[45]
PVDF	8~22	24~34	-	-	-	
P(VDF-TrFE)	12	38	-	-	-	
P(VDF-HFP)	30	24	-	-	-	
P(VDF-CTFE)	-	140	-	-	-	

. Research and Improvement of Piezoelectric Modes

The PEHs depend on the direct piezoelectric effect to convert vibration energy to electrical energy. According to the relationship between the stress and polarization direction of the piezoelectric material, the piezoelectric modes of the PEHs can be divided into d31, d33 and d15 [46–48]. The piezoelectric material is exposed to bending stress when the PEH is operated in d31 and d33 mode. By contrast, the piezoelectric material is exposed to torsion stress when the PEH is operated in d15 mode.

2.3.1. Piezoelectric Energy Harvesters in d31 and d33 Mode

The PEHs possess parallel plate electrodes in d31 mode with the direction of polarization perpendicular to the direction of applied stress. By contrast, a d33 mode PEH is covered with the interdigital electrodes. In addition, the polarization direction is parallel to the direction of applied stress. Furthermore, the device in d33 mode has relatively complex structure compared with d31. The electrode configurations and poling direction of the d31 devices and the d33 devices are, respectively, shown in Figures 3 and 4.

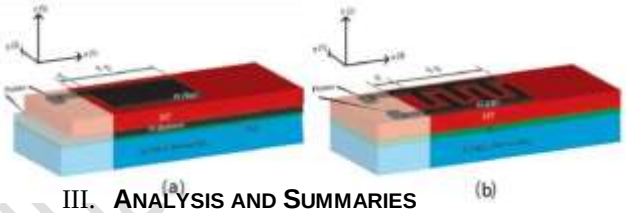

III. Analysis and Summaries

The core of the piezoelectric energy harvester is the piezoelectric material, and recently the common piezoelectric material is piezoelectric ceramics. Piezoelectric ceramics develop towards the lead-free direction while improving the performance. Many researchers have used synthetic materials to optimize and enhance the piezoelectric ceramics. This means that traditional piezoelectric ceramics are composited with some new material with high piezoelectric constant and dielectric permittivity. The piezoelectric material has a promising future because of the diversity of composite materials. Another way to improve the performance of piezoelectric materials is doping. Doping can improve the Curie temperature and the quality of grain growth, but d33 and K_p will be slightly reduced. Furthermore, it will not only affect the dielectric permittivity and piezoelectric constant, but also its lattice constant and phase. The materials are mainly prepared by mixed oxidation, solid-state reaction sintering techniques and SPS. The sintering temperatures of these methods are various. The SPS has many characteristics such as low sintering temperature, low Curie temperature and high cost. By contrast, the traditional method is low cost, but the quality of the prepared material is worse than SPS. The improvement of material properties can directly affect the overall efficiency and stability of the system so the study of piezoelectric materials is a way to enhance the PEH.d31 and d33 are two common piezoelectric modes. The d31 polarization direction and stress direction of piezoelectric materials are perpendicular to each other, while the

polarization direction and stress direction of piezoelectric materials are parallel to each other for d33. The output power in d33 is generally lower than that in d31 because of "dead area" effect. However, by optimizing the electrode width and electrode spacing in d33, the "dead area" proportion will be reduced and its output power can be greatly enhanced. Therefore, the output power in d33 mode has larger scope to be enhanced. Moreover, higher output voltage reduces the energy loss in rectifier circuit. Compared to the d31 and d33 modes, PEHs in d15 mode can generate higher output power. However, they are less applied due to the complexity of fabrication.

Frequency up-conversion is a hot method applied in PEHs in recent years. Its basic principle is to apply the external excitation of high amplitude and low frequency on PEHs of high frequency. Current research shows that the frequency up-conversion method can improve the output power of the PEHs. However, it can cause some energy loss because the implementation process of this method involves collisions. Therefore, its conversion efficiency is still a challenge.

At present, expanding the bandwidth of the PEHs is a popular research method to solve the random changes of external incentive. For the traditional cantilever PEH, the expansion of its bandwidth has the following methods: (1) restricting the displacement of the proof mass; (2) adding the spring force or magnetic force to construct a nonlinear system; and (3) imposing a certain preload to the mass. Although restricting the displacement of the mass or applying a preload to the mass can somewhat expand the operating frequency of the PEH, the maximum output power and output voltage of the PEH are also significantly reduced. The use of nonlinear system can expand the bandwidth of the energy harvester and ensure the output power as well as output voltage.

IV. PROSPECT

To improve the output efficiency of the MEMS scale PEHs, it is possible to start from the aspects of the piezoelectric materials, the piezoelectric modes and the structure of the energy harvester. At present, the piezoelectric material is developing towards the lead-free and high-voltage coefficient direction. In general, compositing material is used to improve the piezoelectric constant and dielectric permittivity of the material while reducing the Curie temperature and the difficulty of sintering. The preparation methods of the material also have a great influence on the quality and parameters of the material. The SPS method can be used in the laboratory research, but the cost of large-scale preparation is high. By contrast, the mixed oxide and solid-state liquid-phase sintering technique are more suitable for industrial production in the future. For the sake of simplicity in the manufacturing process, most piezoelectric energy harvesters take d31 mode electrodes, while the thickness of the piezoelectric material is thin in MEMS devices so the electrode with the d33 mode can provide a higher voltage. This also reduces the energy lost during the collection process through the rectifier circuit. Therefore, the d33 mode should be mainly studied in the energy harvester. However, there is no report about combining d31 with d33, which may be a promising piezoelectric mode in the future. As to a larger energy harvester, d15 mode should be considered due to its higher power harvesting efficiency. Besides, the fabrication of d15 mode device still needs to be optimized. Furthermore, the choice of energy harvester structure depends on the environment. Reducing the resonant frequency of the PEH and up-converting the frequency can be chosen to match the resonant frequency and external excitation of the PEHs for external excitation with relatively concentrated frequency. The frequency bandwidth of the PEHs should be expanded for many non-fixed external frequencies. This means that nonlinear structure will be a better choice to get higher conversion efficiency. In addition, if the harvester structure is designed to be adjustable in frequency, it can also improve the energy efficiency of the PEH combined with the negative feedback system. To harvest the maximum power from PEH, the interface circuit should be carefully designed to achieve impedance matching for the PEH.

ACKNOWLEDGMENT

This work was supported by the National Natural Science Foundation of China: 61741406 and 51702249. The authors would like to thank the valuable advices of the reviewers for this review.

REFERENCES

1. Puccinelli, D.; Haenggi, M. Wireless sensor networks: Applications and challenges of ubiquitous sensing. IEEE Circuits Syst. Mag. **2005**, 5, 19–31. [CrossRef]
2. Rault, T.; Bouabdallah, A.; Challal, Y.; Marin, F. A survey of energy-efficient context recognition systems using wearable sensors for healthcare applications. Pervasive Mob. Comput. **2017**, 37, 23–44. [CrossRef]
3. Park, G.; Farrar, C.R.; Todd, M.D.; Hodgkiss, W.; Rosing, T. Energy harvesting for structural health monitoring sensor networks. J. Infrastruct. Syst. **2007**, 14, 64–79. [CrossRef]
4. Brownfield, M.I.; Mehrjoo, K.; Fayez, A.S.; Iv, N.J.D. Wireless sensor network energy-adaptive MAC protocol. In Proceedings of the 3rd IEEE Consumer Communications and Networking

Conference (CCNC), Las Vegas, NV, USA, 8–10 January 2006; pp. 778–782.
5. Rashid, B.; Rehmani, M.H. Applications of wireless sensor networks for urban areas: A survey. J. Netw. Comput. Appl. **2016**, 60, 192–219. [CrossRef]
6. Vullers, R.J.M.; Van Schaijk, R.; Visser, H.J.; Penders, J.; Van Hoof, C. Energy harvesting for autonomous wireless sensor networks. IEEE Solid-State Circuits Mag. **2010**, 2, 29–38. [CrossRef]
7. Mateu, L.; Moll, F. Review of energy harvesting techniques and applications for microelectronics. In VLSI Circuits and Systems II, Pts 1 and 2; Lopez, J.F., Fernandez, F.V., LopezVillegas, J.M., DelaRosa, J.M., Eds.; Spie-Int Soc Optical Engineering: Bellingham, WA, USA, 2005; Volume 5837, pp. 359–373.
8. Hu, Y.; Wang, Z.L. Recent progress in piezoelectric nanogenerators as a sustainable power source in self-powered systems and active sensors. Nano Energy **2015**, 14, 3–14. [CrossRef]
9. Naifar, S.; Bradai, S.; Viehweger, C.; Kanoun, O. Survey of electromagnetic and magnetoelectric vibration energy harvesters for low frequency excitation. Measurement **2017**, 106, 251–263. [CrossRef]
10. Remick, K.; Quinn, D.D.; McFarland, D.M.; Bergman, L.; Vakakis, A. High-frequency vibration energy harvesting from impulsive excitation utilizing intentional dynamic instability caused by strong nonlinearity. J. Sound Vib. **2016**, 370, 259–279. [CrossRef]
11. Tian, W.C.; Chen, Z.Q.; Cao, Y.R. Analysis and test of a new mems micro-actuator. Microsyst. Technol. **2016**, 22, 943–952. [CrossRef]
12. Tvedt, L.G.W.; Nguyen, D.S.; Halvorsen, E. Nonlinear behavior of an electrostatic energy harvester under wide- and narrowband excitation. J. Microelectromech. Syst. **2010**, 19, 305–316. [CrossRef]
13. Pillatsch, P.; Xiao, B.L.; Shashoua, N.; Gramling, H.M.; Yeatman, E.M.; Wright, P.K. Degradation of bimorph piezoelectric bending beams in energy harvesting applications. Smart Mater. Struct. **2017**, 26, 035046. [CrossRef]
14. El-Sayed, A.R.; Tai, K.; Biglarbegian, M.; Mahmud, S.; IEEE. A survey on recent energy harvesting mechanisms. In Proceedings of the 2016 IEEE Canadian Conference on Electrical and Computer Engineering (CCECE), Vancouver, BC, Canada, 15–18 May 2016; IEEE: New York, NY, USA, 2016.
15. Kholkin, A.; Amdursky, N.; Bdikin, I.; Gazit, E.; Rosenman, G. Strong piezoelectricity in bioinspired peptide nanotubes. ACS Nano **2010**, 4, 610–614. [CrossRef] [PubMed]
16. Malakooti, M.H.; Patterson, B.A.; Hwang, H.S.; Sodano, H.A. Zno nanowire interfaces for high strength multifunctional composites with embedded energy harvesting. Energy Environ. Sci. **2016**, 9, 634–643. [CrossRef]
17. Wang, Z.L. Triboelectric nanogenerators as new energy technology for self-powered systems and as active mechanical and chemical sensors. ACS Nano **2013**, 7, 9533–9557. [CrossRef] [PubMed]
18. Gasnier, P.; Willemin, J.; Chaillout, J.J.; Condemine, C.; Despesse, G.; Boisseau, S.; Gouvernet, G.; Barla, C. Power conversion and integrated circuit architecture for high voltage piezoelectric energy harvesting. Proccedings of the 2012 IEEE 10th International New Circuits and Systems Conference (NEWCAS), Montreal, QC, Canada, 17–20 June 2012; pp. 377–380.
19. Tian, W.C.; Chen, Z.Q. Analysis of a double-phase regulation and an ultra wideband tunable micro electromechanical system resonator. In Proceedings of the 2015 16th International Conference on Electronic Packaging Technology (ICEPT), Changsha, China, 11–14 August 2015; pp. 1149–1153.
20. Hosseinloo, A.H.; Turitsyn, K. Non-resonant energy harvesting via an adaptive bistable potential. Smart Mater. Struct. **2016**, 25, 015010. [CrossRef]
21. Andò, B.; Baglio, S.; Bulsara, A.R.; Marletta, V.; Pistorio, A. Investigation of a nonlinear energy harvester. IEEE Trans. Instrum. Meas. **2017**, 66, 1067–1075. [CrossRef]
22. Iannacci, J.; Sordo, G.; Serra, E.; Schmid, U. The mems four-leaf clover wideband vibration energy harvesting device: Design concept and experimental verification. Microsyst. Technol. **2016**, 22, 1865–1881. [CrossRef]
23. Sodano, H.A.; Park, G.; Inman, D.J. Estimation of electric charge output for piezoelectric energy harvesting. Strain **2004**, 40, 49–58. [CrossRef]

24. Williams, C.; Yates, R.B. Analysis of a micro-electric generator for microsystems. Sens. Actuator A Phys. **1996**, 52, 8–11. [CrossRef]
25. Roundy, S.; Wright, P.K.; Rabaey, J. A study of low level vibrations as a power source for wireless sensor nodes. Comput. Commun. **2003**, 26, 1131–1144. [CrossRef]
26. Koptsik, V.A.; Rez, I.S. From the history of physics: Pierre curie's works in the field of crystal physics (on the one-hundredth anniversary of the discovery of the piezoelectric effect). Sov. Phys. Uspekhi **1981**, 24, 426. [CrossRef]
27. Damjanovic, D. Ferroelectric, dielectric and piezoelectric properties of ferroelectric thin films and ceramics. Rep. Prog. Phys. **1998**, 61, 1267–1324. [CrossRef]
28. Bernstein, J.J.; Bottari, J.; Houston, K.; Kirkos, G.; Miller, R.; Xu, B.; Ye, Y.; Cross, L.E. Advanced mems ferroelectric ultrasound 2D arrays. In Proceedings of the 1999 IEEE Ultrasonics Symposium, Caesars Tahoe, NV, USA, 17–20 October 1999; Schneider, S.C., Levy, M., McAvoy, B.R., Eds.; IEEE: New York, NY, USA, 1999; pp. 1145–1153.
29. Tressler, J.F.; Alkoy, S.; Newnham, R.E. Piezoelectric sensors and sensor materials. J. Electroceram. **1998**, 2, 257–272. [CrossRef]
30. Kawai, H. The piezoelectricity of poly (vinylidene fluoride). Jpn. J. Appl. Phys. **1969**, 8, 975. [CrossRef]
31. Zeng, W.; Tao, X.M.; Chen, S.; Shang, S.M.; Chan, H.L.W.; Choy, S.H. Highly durable all-fiber nanogenerator for mechanical energy harvesting. Energy Environ. Sci. **2013**, 6, 2631–2638. [CrossRef]
32. Soin, N.; Shah, T.H.; Anand, S.C.; Geng, J.F.; Pornwannachai, W.; Mandal, P.; Reid, D.; Sharma, S.; Hadimani, R.L.; Bayramol, D.V.; et al. Novel "3-D spacer" all fibre piezoelectric textiles for energy harvesting applications. Energy Environ. Sci. **2014**, 7, 1670–1679. [CrossRef]
33. Takenaka, T.; Okuda, T.; Takegahara, K. Lead-free piezoelectric ceramics based on $(Bi_{1/2}Na_{1/2})TiO_3$-$NaNbO_3$. Ferroelectrics **1997**, 196, 175–178. [CrossRef]
34. Guo, Y.; Kakimoto, K.I.; Ohsato, H. $(Na_{0.5}K_{0.5})NbO_3$–$LiTaO_3$ lead-free piezoelectric ceramics. Mater. Lett. **2005**, 59, 241–244. [CrossRef]
35. Li, J.F.; Wang, K.; Zhang, B.P.; Zhang, L.M. Ferroelectric and piezoelectric properties of fine-grained Na0.5K0.5NbO_3 lead-free piezoelectric ceramics prepared by spark plasma sintering. J. Am. Ceram. Soc. **2006**, 89, 706–709. [CrossRef]
36. Lin, D.; Xiao, D.; Zhu, J.; Yu, P. Piezoelectric and ferroelectric properties of $[Bi_{0.5}(Na_{1-x-y}K_xLi_y)_{0.5}]TiO_3$ lead-free piezoelectric ceramics. Appl. Phys. Lett. **2006**, 88, 062901. [CrossRef]
37. Lin, Y.; Zhang, L.; Yu, J. Piezoelectric and ferroelectric property in Mn-doped $0.69BiFeO_3$–$0.04Bi(Zn_{1/2}Ti_{1/2})O_3$–$0.27BaTiO_3$ lead-free piezoceramics. J. Mater. Sci.-Mater. Electron. **2016**, 27, 1955–1965. [CrossRef]
38. Cheng, C.M.; Pei, C.H.; Chen, M.L.; Chen, K.H. The inferences of ZnO additions for LKNNT lead-free piezoelectric ceramics. Integr. Ferroelectr. **2016**, 168, 61–68. [CrossRef]
39. Shi, J.; Tian, W.; Liu, X.; Fan, H. Electric-field induced phase transition and fatigue behaviors of $(Bi_{0.5+x/2}Na_{0.5-x/2})_{0.94}Ba_{0.06}Ti_{1-x}Fe_xO_3$ ferroelectrics. J. Am. Ceram. Soc. **2017**, 100, 1080–1090. [CrossRef]
40. Koruza, J.; Rojas, V.; Molina-Luna, L.; Kunz, U.; Duerrschnabel, M.; Kleebe, H.J.; Acosta, M. Formation of the core–shell microstructure in lead-free $Bi_{1/2}Na_{1/2}TiO_3$-$SrTiO_3$ piezoceramics and its influence on the electromechanical properties. J. Eur. Ceram. Soc. **2016**, 36, 1009–1016. [CrossRef]
41. Martins, P.; Lopes, A.C.; Lanceros-Mendez, S. Electroactive phases of poly(vinylidene fluoride): Determination, processing and applications. Prog. Polym. Sci. **2014**, 39, 683–706. [CrossRef]
42. Kornphom, C.; Vittayakorn, N.; Bongkarn, T. Lead-free piezoelectric ceramics based on (1 x)BNKLLT–xBCTZ binary solid solutions synthesized by the solid-state combustion technique. J. Mater. Sci. **2016**, 51, 4142–4149. [CrossRef]
43. Machado, R.; Santos, V.B.D.; Ochoa, D.A.; Cerdeiras, E.; Mestres, L.; García, J.E. Elastic, dielectric and electromechanical properties of $(Bi_{0.5}Na_{0.5})TiO_3$-$BaTiO_3$ piezoceramics at the morphotropic phase boundary region. J. Alloys Compd. **2017**, 690, 568–574. [CrossRef]
44. Weng, C.-M.; Tsai, C.-C.; Hong, C.-S.; Sheen, J.; Chu, S.-Y.; Tang, J.-F.; Zou, Y.-H. Effects of LiNbO3-doping on properties of $(Na_{0.535}K_{0.48})NbO_3$ piezoelectric ceramics with high electromechanical coupling coefficient for application in surface acoustic wave devices. Ceram. Int. **2017**, 43, 11324–11330. [CrossRef]
45. Chen, Y.; Xue, D.; Chen, Z.; Jiang, X.; Gou, J.; Liu, G.; Liu, X.; Xu, Z. Lithium-modified $(K_{0.5}Na_{0.5})NbO_3$–$BiAlO_3$ lead-free piezoelectric ceramics with high curie temperature. Ceram. Int. **2017**, 43, 634–640. [CrossRef]

46. Chhabra, P.; Sharma, A.; Krishna, N.P.V. Fabrication and characterisation of bulk micromachined zno energy transducer with interdigitated electrodes. Microsyst. Technol. **2016**, 22, 1055–1066. [CrossRef]
47. Deng, L.; Wen, Z.; Zhao, X.; Yuan, C.; Luo, G.; Mo, J. High voltage output mems vibration energy harvester in d_{31} mode with pzt thin film. J. Microelectromech. Syst. **2014**, 23, 855–861. [CrossRef]
48. Kulkarni, V.; Ben-Mrad, R.; Prasad, S.E. A torsion based shear mode piezoelectric energy harvester for wireless sensor modules. In Proceedings of the ASME 2014 International Mechanical Engineering Congress and Exposition, Montreal, QC, Canada, 14–20 November 2014; p. V04BT04A053.
49. Sherman, C.H.; Butler, J.L. Transducers and arrays for underwater sound. J. Acoust. Soc. Am. **2008**, 124, 1385.
50. Kim, S.B.; Park, H.; Kim, S.H.; Wikle, H.C.; Park, J.H.; Kim, D.J. Comparison of mems pzt cantilevers based on d_{31} and d_{33} modes for vibration energy harvesting. J. Microelectromech. Syst. **2013**, 22, 26–33. [CrossRef]
51. Bowen, C.R.; Nelson, L.J.; Stevens, R.; Cain, M.G.; Stewart, M. Optimisation of interdigitated electrodes for piezoelectric actuators and active fibre composites. J. Electroceram. **2006**, 16, 263–269. [CrossRef]
52. Chidambaram, N.; Mazzalai, A.; Balma, D.; Muralt, P. Comparison of lead zirconate titanate thin films for microelectromechanical energy harvester with interdigitated and parallel plate electrodes. IEEE Trans. Ultrason. Ferroelectr. Freq. Control **2013**, 60, 1564. [CrossRef] [PubMed]
53. Gevorgian, S.S.; Martinsson, T.; Linner, P.L.J.; Kollberg, E.L. Cad models for multilayered substrate interdigital capacitors. IEEE Trans. Microw. Theory Tech. **1996**, 44, 896–904. [CrossRef]
54. Yang, S.; Dong, W.; Wang, D.; Yin, X. Study of complete interdigital electrode d_{33} mode piezoelectric cantilever energy harvester. Transducer Microsyst. Technol. **2015**, 34, 52–55.
55. Cho, H.; Park, J.; Park, J.Y. Micro-fabricated flexible pzt cantilever using d_{33} mode for energy harvesting. Micro Nano Syst. Lett. **2017**, 5, 20. [CrossRef]
56. Kim, H.; Tadesse, Y.; Priya, S. Piezoelectric energy harvesting. In Energy Harvesting Technologies; Priya, S., Inman, D.J., Eds.; Springer: Boston, MA, USA, 2009; pp. 3–39.
57. Malakooti, M.H.; Sodano, H.A. Shear mode energy harvesting of piezoelectric sandwich beam. In Active and Passive Smart Structures and Integrated Systems 2013; Sodano, H.A., Ed.; Spie-Int Soc Optical Engineering: Bellingham, WA, USA, 2013; Volume 8688.
58. Malakooti, M.H.; Sodano, H.A. Piezoelectric energy harvesting through shear mode operation. Smart Mater. Struct. **2015**, 24, 055005. [CrossRef]
59. Abdelkefi, A.; Najar, F.; Nayfeh, A.H.; Ben Ayed, S. An energy harvester using piezoelectric cantilever beams undergoing coupled bending-torsion vibrations. Smart Mater. Struct. **2011**, 20, 115007. [CrossRef]
60. Gao, S.; Zhang, G.; Jin, L.; Li, P.; Liu, H. Study on characteristics of the piezoelectric energy-harvesting from the torsional vibration of thin-walled cantilever beams. Microsyst. Technol. **2017**, 23, 5455–5465. [CrossRef]
61. Kulkarni, V.; Ben-Mrad, R.; Prasad, S.E.; Nemana, S. A shear-mode energy harvesting device based on torsional stresses. IEEE/ASME Trans. Mechatron. **2014**, 19, 801–807. [CrossRef]
62. Ferrari, M.; Ferrari, V.; Guizzetti, M.; Andò, B.; Baglio, S.; Trigona, C. Improved energy harvesting from wideband vibrations by nonlinear piezoelectric converters. Sens. Actuator A Phys. **2010**, 162, 425–431. [CrossRef]
63. Liu, H.; Lee, C.; Kobayashi, T.; Tay, C.J.; Quan, C. A new S-shaped MEMS PZT cantilever for energy harvesting from low frequency vibrations below 30 Hz. Microsyst. Technol. **2012**, 18, 497–506. [CrossRef]
64. Zhang, L.; Lu, J.; Takei, R.; Makimoto, N.; Itoh, T.; Kobayashi, T. S-shape spring sensor: Sensing specific low-frequency vibration by energy harvesting. Rev. Sci. Instrum. **2016**, 87, 085005. [CrossRef] [PubMed]
65. Karami, M.A.; Inman, D.J. Electromechanical modeling of the low-frequency zigzag micro-energy harvester. J. Intell. Mater. Syst. Struct. **2011**, 22, 271–282. [CrossRef]
66. Kim, I.H.; Jin, S.S.; Jang, S.J.; Jung, H.J. A performance-enhanced energy harvester for low frequency vibration utilizing a corrugated

cantilevered beam. Smart Mater. Struct. **2014**, 23, 623–626. [CrossRef]

67. Kulah, H.; Najafi, K. Energy scavenging from low-frequency vibrations by using frequency up-conversion for wireless sensor applications. IEEE Sens. J. **2008**, 8, 261–268. [CrossRef]
68. Chen, S.; Ma, L.; Chen, T.; Liu, H.; Sun, L.; Wang, J. Modeling and verification of a piezoelectric frequency-up-conversion energy harvesting system. Microsyst. Technol. **2017**, 23, 2459–2466. [CrossRef]
69. Kwon, D.S.; Ko, H.J.; Kim, J. Piezoelectric and electromagnetic hybrid energy harvester using two cantilevers for frequency up-conversion. In Proceedings of the IEEE International Conference on MICRO Electro Mechanical Systems, Las Vegas, NV, USA, 22–26 January 2017.
70. Halim, M.A.; Park, J.Y. A non-resonant, frequency up-converted electromagnetic energy harvester from human-body-induced vibration for hand-held smart system applications. J. Appl. Phys. **2014**, 115, 094901. [CrossRef]
71. Halim, M.A.; Park, J.Y. Piezoelectric energy harvester using impact-driven flexible side-walls for human-limb motion. Microsyst. Technol. **2018**, 24, 2099–2107. [CrossRef]
72. Jeong, S.W.; Yoo, H.H. Bi-stable cantilevered piezoelectric energy harvester using springs. In Proceedings of the 23rd International Congress on Sound and Vibration: From Ancient to Modern Acoustics, Athens, Greece, 10–14 July 2016; Vogiatzis, K., Kouroussis, G., Crocker, M., Pawelczyk, M., Eds.; International Institute Acoustics & Vibration: Auburn, AL, USA, 2016.
73. Braghin, F.; Mehdipour, I.; Lecis, N.; Galassi, C. Periodic substructure for multi-frequency energy harvesting with single piezoelectric patch. In Active and Passive Smart Structures and Integrated Systems 2016; Park, G., Ed.; Spie-Int Soc Optical Engineering: Bellingham, WA, USA, 2016; Volume 9799.
74. Yang, W.; Towfighian, S. A hybrid nonlinear vibration energy harvester. Mech. Syst. Signal Process. **2017**, 90, 317–333. [CrossRef]
75. Wang, X.; Chen, C.; Wang, N.; San, H.; Yu, Y.; Halvorsen, E.; Chen, X. A frequency and bandwidth tunable piezoelectric vibration energy harvester using multiple nonlinear techniques. Appl. Energy **2017**, 190, 368–375. [CrossRef]
76. Bao, M.; Yang, H. Squeeze film air damping in mems. Sens. Actuator A Phys. **2007**, 136, 3–27. [CrossRef]
77. Schmidt, V.H. Theoretical electrical power output per unit voume of PVF_2 and mechanical-to-electrical conversion efficiency as functions of frequency. In Proceedings of the 6th IEEE International Symposium on Applications of Ferroelectrics, Bethlehem, PA, USA, 8–11 June 1986; pp. 538–542.